FLYBACK VS. FORWARD CONVERTER TOPOLOGY COMPARISON BASED UPON MAGNETIC DESIGN

Hernán Emilio TACCA

Universidad de Buenos Aires , Facultad de Ingeniería
LABCATYP - Depto. de Electrónica
htacca@fi.uba.ar

***Abstract* - Based on approximative equations for single step calculation design procedures, a simple method useful to adopt the most suitable topology in low power DC to DC conversion is derived from the volume calculation of the magnetic cores needed.**

***Index terms* - Low power magnetic components, switching power converters, flyback and forward magnetics design.**

NOMENCLATURE

B_{max}	peak value of the induction
B_{min}	induction minimum value
D	duty-cycle factor
f	switching frequency
$F_{c_{P/S}}$	window filling factor of the primary/secondary coil (also known as copper factor) : $F_{c_{P/S}} = n_{P/S}\ S_{Cu_{P/S}} / S_{W_{P/S}}$
f_{f_V}	voltage form factor
F_P	partition factor of the primary windings : $F_P = S_{W_P} / S_W$
f_{pr}	power switch profit factor (or power device utilization factor)
F_r	total winding eddy currents factor
F_W	window factor : $F_W = S_W / S_{Fe}$
$I_{L_{av}}$	average value of the inductor current
$I_{L_{ef}}$	effective value of the inductor current
$I_{L_{max}}$	peak value of the inductor current
$I_{P_{av}}$	average value of the primary current
$I_{P_{ef}}$	effective value of the primary current
$I_{P_{max}}$	peak value of the primary current
k_C	core sizing characteristic converter topology coefficient
k_{ES}	effective core shape factor
k_{rS}	skin effect factor
k_{rX}	proximity effect factor
k_S	geometrical core shape factor
k_{u_T}	transformer utilization factor
L	inductance of the smoothing inductor
l_a	air gap
$l_{e_{av}}$	average mean turn length
l_{em}	mean turn length
l_{Fe}	effective magnetic length
n_P	primary turns
n_S	secondary turns
P_{Cu}	winding losses
P_D	device rated switching power
P_{Fe}	core losses
P_O	converter output power
R_{ac}	a.c. resistance
R_{dc}	d.c. resistance
$\Re \boldsymbol{V}_{FW/FB}$	total forward core volume to flyback core volume ratio
R_θ	thermal resistance
S_{Cu_L}	inductor wire cross section
S_{Cu_P}	primary wire cross section
S_{Cu_S}	secondary wire cross section
S_{dis}	heat dissipation surface
S_{Fe}	minimum core section
$S_{Fe\,ef}$	effective core section
$S_{Fe_{FB}}$	flyback core section required
S_{Fe_L}	inductor core section required
$S_{Fe_{TFW}}$	forward transformer core section required
S_W	window area
S_{W_P}	primary window area
S_{W_S}	secondary window area
t_C	power switch conduction time
$\boldsymbol{V}_{Fe_{FB}}$	core volume of the flyback coupled inductor (usually named flyback "*transformer*")
$\boldsymbol{V}_{Fe_{FW}}$	total volume occupied by the cores of the forward converter
$\boldsymbol{V}_{Fe_L}$	core volume of the smoothing inductor
$\boldsymbol{V}_{Fe_{TFW}}$	core volume of the forward transformer
V_P	primary supply voltage
Δ	penetration depth

ΔB	maximum induction increment
δi_L	normalized amplitude of the inductor ripple current
δi_P	normalized primary current variation
η	converter efficiency
Φ	magnetic flux
μ_o	magnetic field constant
μ_{rs}	relative static permeability (derived from the static magnetization curve)
ρ	conductor resistivity
σ_L	inductor current density
σ_P	primary current density

I. INTRODUCTION

In DC to DC converters and off-line switching power supplies for low power applications, the most used topologies are the flyback and the forward converters [1].

The flyback structure has the advantage of requiring only a single magnetic component. This one, if designed for minimum size, results smaller than the overall volume occupied by both the smoothing inductor plus the power transformer of the equivalent forward converter. However, when the flyback coupled inductor size is minimum, the profit factor of the power switch becomes poor [2][3]. If an improved profit of the flyback power device is required, it results mandatory to supersize the magnetic component . So, a trade-off arises between the core size and the rated switching power (maximum theoretical switching power) of the power transistor [4]. The better the profit factor, heavier the magnetic cores become and this apply to both topologies here compared. Nevertheless, the required core volumes result from different laws, so for a wanted profit factor, one topology will be the most suitable regarding the core weight.

In this work, the total magnetic material volume required for both alternatives are computed and related. The comparison criterion is stated as the ratio of core sizing approximative equations, which become justified by the closed matching with results obtained using manufacturer design data and recommended procedures.

Derivation of some equations involved on design procedures are presented in appendices (including some application examples agreeing with manufacturer data).

In order to compare topologies, first, the required core sections are obtained and then, the core volumes are computed assuming identical core shapes for all the magnetic components involved.

Finally, the volume rate is plotted to bring an easy method to know wich topology will be the lightest.

II. FLYBACK CONVERTER

A. Basic flyback circuit

Fig. 1.a depicts the basic circuit of a flyback converter and fig. 1.b shows the corresponding waveforms. From fig. 1.b it may be defined :

$$\Delta I_P = I_{P_{max}} - I_{P_{min}} \tag{2.1}$$

$$\delta i_P = \Delta I_P / I_{P_{max}} \tag{2.2}$$

$$D = t_C / T \tag{2.3}$$

and from the current waveforms it follows :

$$I_{P_{av}} = D\, I_{P_{max}} \left(1 - \frac{\delta i_P}{2}\right) \tag{2.4}$$

$$I_{P_{ef}} = \sqrt{D}\; I_{P_{max}} \sqrt{1 - \delta i_P + \frac{1}{3}\delta {i_P}^2} \tag{2.5}$$

Then, the output power is :

$$P_O = \eta\, P_P = \eta V_P\; I_{P_{av}} = \eta\, D\left(1 - \frac{\delta i_P}{2}\right) V_P\; I_{P_{max}} \tag{2.6}$$

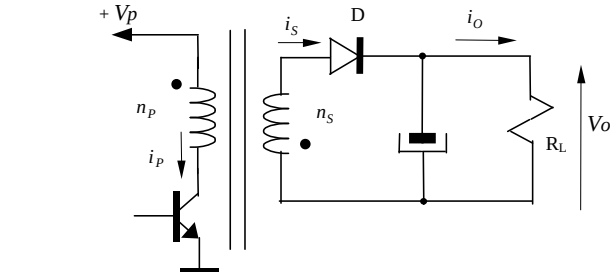

(a)

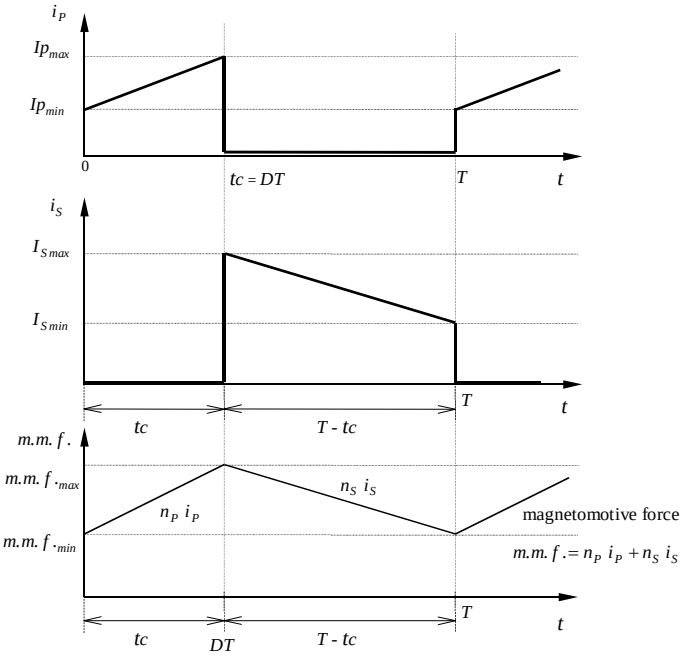

(b)

Figure 1 : Flyback converter, *(a)* basic circuit, *(b)* basic waveforms.

B. Core sizing

The primary current density is :

$$\sigma_P = \frac{I_{P_{ef}}}{S_{Cu_P}} \tag{2.7}$$

where S_{Cu_P} is the cross section of the primary wire that must verify :

$$S_{Cu_P} = F_P\; F_{c_P}\; S_W / n_P \tag{2.8}$$

In accordance with the Faraday law :

$$V_P = n_P \frac{\Delta B}{t_C} S_{Fe} \tag{2.9}$$

where, $\Delta B = B_{max} - B_{min}$ and

$$B_{max} = \frac{\mu_o}{l_a + \frac{l_{Fe}}{\mu_{rs}}} n_P \; I_{P_{max}} \cong \frac{\mu_o}{l_a} n_P \; I_{P_{max}} \tag{2.10}$$

because usually :

$$l_a >> l_{Fe}/\mu_{rs}$$

where μ_{rs} is the relative static permeability.

By a similar way,

$$\Delta B \cong \frac{\mu_o}{l_a} n_P \; \Delta I_P \tag{2.11}$$

Relating 2.10 and 2.11 yields :

$$\frac{\Delta B}{B_{max}} = \frac{\Delta I_P}{I_{P_{max}}} = \delta i_P \tag{2.12}$$

using this equation (with the simplified notation $B_m = B_{max}$) the expression 2.9 yields :

$$V_P = n_P \; \delta i_P \; B_m \frac{f}{D} S_{Fe} \tag{2.13}$$

With eqs. 2.5 , 2.6 , 2.7 , 2.8 and 2.13 , using the window factor definition $F_W = S_W / S_{Fe}$, it results :

$$S_{Fe_{FB}} = G_{(\delta i_p)} \sqrt{\frac{\sqrt{D} \; P_O}{\eta \; \delta i_P \; B_m \; f \; \sigma_P \; F_{c_P} \; F_P \; F_W}} \tag{2.14.a}$$

where,

$$G_{(\delta i_p)} = \sqrt{\frac{\sqrt{1 - \delta i_P + \frac{1}{3}\delta {i_P}^2}}{\left(1 - \frac{\delta i_P}{2}\right)}} \tag{2.14.b}$$

For all the possible values $0 \le \delta i_P \le 1$ it results $1 \le G_{(\delta i_p)} < 1.075$, so the expression 2.14.a may be simplified assuming $G_{(\delta i_p)} \cong 1$.

To complete the design, it is necessary to adopt the partition factor of the primary windings (see section IV), the primary current density (section V) and the maximum value of the induction (Appendix I).

III. FORWARD CONVERTER

A. Basic circuit and transformer core sizing

The typical circuit of a forward converter is presented in fig. 2.a , while its waveforms are depicted in fig. 2.b . The equation of the primary voltage becomes :

$$V_P = n_P \frac{B_m}{t_C} S_{Fe} = \frac{1}{D} \; n_P \; B_m \; f \; S_{Fe} \tag{3.1}$$

from which, the sizing equation results :

$$S_{Fe_{TFW}} = G_{(\delta i_p)} \sqrt{\frac{\sqrt{D} \; P_O}{\eta \; B_m \; f \; \sigma_P \; F_{c_P} \; F_P \; F_W}} \tag{3.2}$$

where it may be approximated

$$G_{(\delta i_p)} \cong 1$$

as it was done with flyback converters.

The equations 3.1 and 3.2 are particular cases of generalized expressions valid for many other converter topologies (Apendix II).

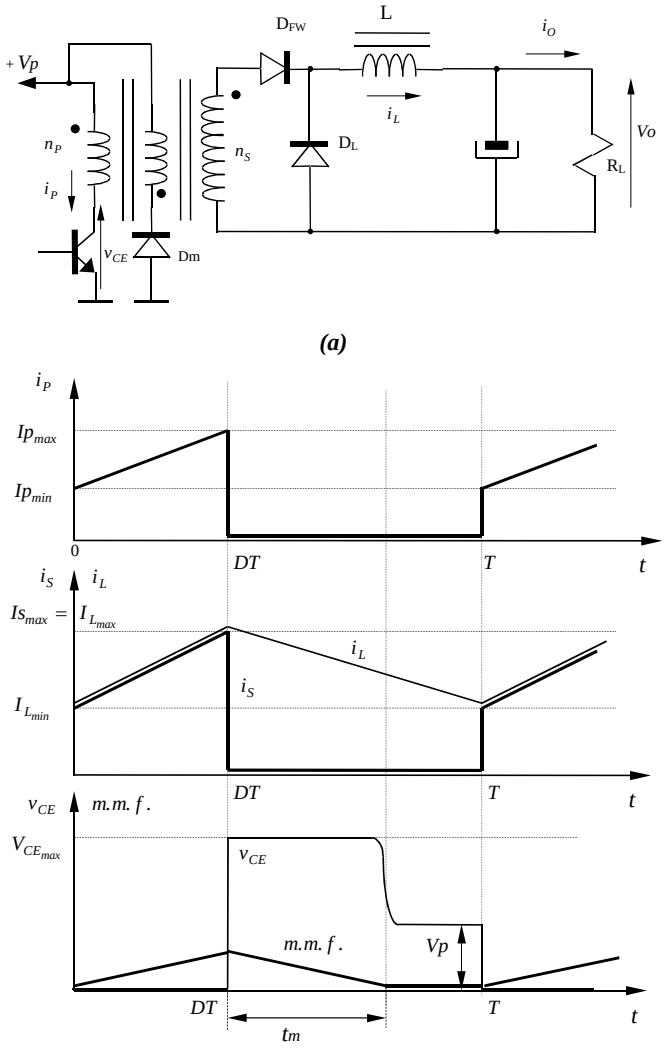

Figure 2 : Forward converter, *(a)* basic circuit, *(b)* basic waveforms.

B. Inductor core sizing

The effective value of the inductor current can be expressed as :

$$I_{L_{ef}} = \sigma_L \; S_{Cu_L} = \sigma_L \; F_c \frac{S_{W_L}}{n_L} = \sigma_L \; F_c \; F_W \frac{S_{Fe_L}}{n_L} \tag{3.3}$$

On the other hand,

$$L = \frac{n_L \; \Phi}{i_L} = \frac{n_L \; B_m \; S_{Fe_L}}{I_{L_{max}}} \tag{3.4}$$

Using eqs. 3.3 and 3.4 :

$$S_{Fe_L} = \sqrt{\frac{L \; I_{L_{ef}} \; I_{L_{max}}}{\sigma_L \; F_c \; F_W \; B_m}} \tag{3.5}$$

From fig. 2.b it follows :

$$I_{L_{ef}} = I_{L_{max}} \sqrt{1-\delta i_L + \frac{1}{3}\delta i_L{}^2} \quad (3.6)$$

$$I_{L_{av}} = I_{L_{max}} \left(1-\frac{\delta i_L}{2}\right) \quad (3.7)$$

and then, the output power results :

$$P_O = V_O\ I_{L_{av}} = \frac{n_S}{n_P} D\left(1-\frac{\delta i_L}{2}\right) V_P\ I_{L_{max}} \quad (3.8)$$

During the interval $0 \le t \le D\,T$ it must be

$$\frac{n_S}{n_P} V_P - V_O = L\frac{\Delta I_L}{D\,T}$$

that may be expressed as

$$(1-D)\frac{n_S}{n_P} = \frac{L\ f}{D\,V_P} I_{L_{max}}\ \delta i_L \quad (3.9)$$

Substituting eqs. 3.6 , 3.8 and 3.9 in 3.5 , yields :

$$S_{Fe_L} = G_{(\delta i_L)} \sqrt{\frac{(1-D)\ P_O}{\delta i_L\ B_m\ f\ \sigma_L\ F_c\ \ F_W}} \quad (3.10)$$

where , as previously stated , it may be aproximated $G_{(\delta i_L)} \cong 1$. Also, it can be assumed that $\delta i_L \cong \delta i_P$ provided that the magnetizing inductance be large enough.

In order to complete the design, the air-gap and the winding turns must be determined, which may be done by several graphical [5][6] or analytical methods [7]-[9][11].

IV. PARTITION FACTOR OF THE WINDING AREA

Optimal partition factor :

The optimum is defined as that value which minimizes the winding losses, given by

$$P_{Cu} = P_{Cu_P} + P_{Cu_S} = I_{P_{ef}}{}^2\ R_{Cu_P} + I_{S_{ef}}{}^2\ R_{Cu_S} \quad (4.1)$$

where, the winding resistances are

$$R_{Cu_P} = \rho_{eq_P}\ n_P\ \frac{l_{em_P}}{S_{Cu_P}} \quad (4.2.a)$$

$$R_{Cu_S} = \rho_{eq_S}\ n_S\ \frac{l_{em_S}}{S_{Cu_S}} \quad (4.2.b)$$

and, $l_{em_{P/S}}$ are the primary and secondary mean turn lengths, while $\rho_{eq_{P/S}}$ are the equivalent resistivities of the primary and secondary conductors, taken into account skin and proximity effects [7][8][12][13] :

$$\rho_{eq_{P/S}} = F_{r_{P/S}}\ \rho_{Cu} \quad (4.2.c)$$

$$F_{r_{P/S}} = k_{rS_{P/S}} + k_{rX_{P/S}} \quad (4.2.d)$$

being $k_{rS_{P/S}}$ the primary and secondary skin effect factors and $k_{rX_{P/S}}$ the proximity factors (Appendix III).

The conductor sections are :

$$S_{Cu_P} = F_P\ F_{c_P}\ \frac{S_W}{n_P} \quad (4.3.a)$$

$$S_{Cu_S} = (1-F_P)\ F_{c_S}\ \frac{S_W}{n_S} \quad (4.3.b)$$

where, $F_{c_{P/S}}$ are respectively, the fill factors of the primary and secondary coils, while F_P is the partition factor of the primary windings defined as the ratio between the window area occupied by the primary winding and the total window area , $F_P = S_{W_P}/S_W$.

Substituting the eqs. 4.3 into eqs. 4.2 , then the result into 4.1, and considering both

$$n_P\ I_{P_{ef}} = n_S\ I_{S_{ef}} \quad \text{and} \quad S_W = F_W\ S_{Fe}\ ,$$

yields :

$$P_{Cu} = \rho_{eq_P}\ \frac{I_{P_{ef}}{}^2\ n_P{}^2}{F_W\ S_{Fe}} \left[\frac{l_{em_P}}{F_{c_P}\ F_P} + \frac{l_{em_S}\left(F_{r_S}/F_{r_P}\right)}{F_{c_S}\ (1-F_P)}\right] \quad (4.4)$$

On the other hand, the current densities in each winding are :

$$\sigma_P = I_{P_{ef}}/S_{Cu_P} \quad \text{and} \quad \sigma_S = I_{S_{ef}}/S_{Cu_S}\ ,$$

that related give :

$$\frac{\sigma_P}{\sigma_S} = \frac{F_{c_S}}{F_{c_P}}\left(\frac{1}{F_P}-1\right) \quad (4.5)$$

Considering the common winding techniques, two alternatives will be studied.

1. Shared coil-former windings

In this case : $l_{em_P} = l_{em_S} = l_{em}$ so , the eq. 4.4 becomes :

$$P_{Cu} = \rho_{eq_P}\ I_{P_{ef}}{}^2\ n_P{}^2\ \frac{l_{em}}{F_W\ S_{Fe}} \left[\frac{1}{F_{c_P}\ F_P} + \frac{\left(F_{r_S}/F_{r_P}\right)}{F_{c_S}\ (1-F_P)}\right] \quad (4.6)$$

The optimal partition factor will be the one which minimizes the copper losses given by eq. 4.6 . That is :

$$F_{P_{opt}} = \frac{1}{1+\sqrt{\frac{F_{c_P}}{F_{c_S}}\frac{F_{r_S}}{F_{r_P}}}} \quad (4.7)$$

and from eq. 4.5 , the current densities become related by :

$$\frac{\sigma_P}{\sigma_S} = \sqrt{\frac{F_{c_S}}{F_{c_P}}\frac{F_{r_S}}{F_{r_P}}} \quad (4.8)$$

For the particular case when $F_{c_P} = F_{c_S}$ and $F_{r_P} = F_{r_S}$ it results :

$$F_{P_{opt}} = \frac{1}{2} \quad (4.9.a)$$

and

$$\sigma_P = \sigma_S \quad (4.9.b)$$

In such a case, the Joule losses result :

$$P_{Cu} = \rho_{eq_P}\ I_{P_{ef}}{}^2\ n_P{}^2\ \frac{4\ l_{em}}{F_{c_P}\ F_W\ S_{Fe}} \quad (4.10)$$

Defining the equivalent turn factor :

$$F_{le} = \frac{1}{2}\left[1+\frac{F_{c_P}}{F_{c_S}}\frac{F_P}{(1-F_P)}\frac{F_{r_S}}{F_{r_P}}\right] \quad (4.11)$$

the eq. 4.6 may be rewritten as :

$$P_{Cu} = 2\rho_{eq_P}\ I_{P_{ef}}{}^2\ n_P{}^2\ \frac{F_{le}\ l_{em}}{F_P\ F_{c_P}\ F_W\ S_{Fe}} \quad (4.12)$$

where, according to eqs. 4.2.c and 4.2.d , it is

$$\rho_{eq_P} = \left(k_{rS_P} + k_{rX_P}\right) \rho_{Cu}$$

2. Stacked windings

In case of superposed winding sections (for example secondary over primary) the mean turn lengths become different and will depend on the the primary partition factor adopted. For the core of fig. 3.a , according to fig. 3.b , the sectional mean turn lengths will be :

$$l_{em_P} = 2(A+B) + \pi\, C_P \tag{4.13.a}$$

$$l_{em_S} = 2(A+B) + 2\pi\left(C - \frac{C_S}{2}\right) \tag{4.13.b}$$

where :

$$C = C_P + C_S \tag{4.13.c}$$

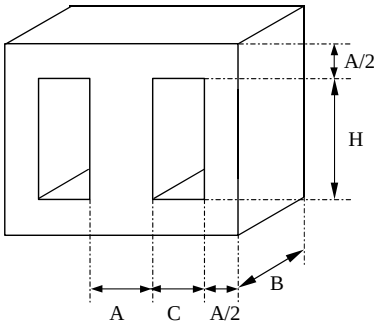

(a)

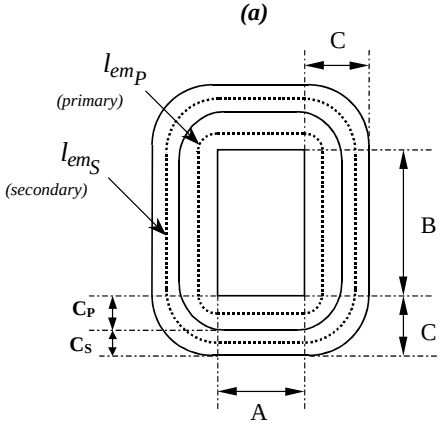

(b)

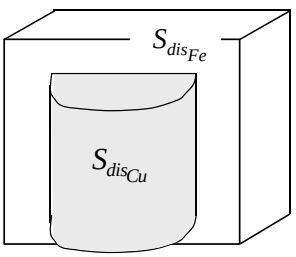

$$S_{dis_{Cu}} = 2\left[(\pi C + A)(H + C) + C\,A\right]$$

$$S_{dis_{Fe}} = 2\left\{(A+B)\left[2(A+C)+H\right] + A\,B\right\}$$

(c)

Figure 3 : E-type core, *(a)* dimensions, *(b)* mean turn lenghts, *(c)* dissipation surfaces.

Defining the average mean turn length as :

$$l_{e_{av}} = \frac{1}{2}\left(l_{em_P} + l_{em_S}\right) \tag{4.14}$$

and using the eq. 4.13 , the definition 4.14 may be expressed as :

$$l_{e_{av}} = 2(A+B) + \pi\, C + \frac{\pi}{2}\left(C_P - C_S\right) \tag{4.15}$$

For $C_P = C_S$ the average mean turn length coincides with the single section mean turn length, defined by :

$$l_{em} = l_{e_{av}}\Big]_{C_P = C_S} = 2(A+B) + \pi\, C \tag{4.16}$$

and from fig. 3.a , the following geometrical coefficients are defined :

$$F_h = H/C \tag{4.17.a}$$

and

$$F_s = B/A \tag{4.17.b}$$

The primary partition factor is :

$$F_P = \frac{S_{W_P}}{S_W} = \frac{C_P}{C} \tag{4.18}$$

where *C* may be expressed by ,

$$C = \sqrt{\frac{F_W}{F_h}}\,\sqrt{S_{Fe}} \tag{4.19}$$

Using eqs. 4.13.c , 4.16 , 4.18 and 4.19 , the eqs. 4.13.a and 4.13.b may be expressed as :

$$l_{em_P} = l_{em} - \pi\sqrt{\frac{F_W}{F_h}}\left(1 - F_P\right)\sqrt{S_{Fe}} \tag{4.20.a}$$

$$l_{em_S} = l_{em} + \pi\sqrt{\frac{F_W}{F_h}}\;F_P\;\sqrt{S_{Fe}} \tag{4.20.b}$$

Substituting 4.20.a and b into 4.4 yields :

$$P_{Cu} = \rho_{eq_P}\; {I_{P_{ef}}}^2\; {n_P}^2\; \frac{l_{em}}{F_W\; S_{Fe}} \cdot \cdot\left[\frac{1 - M\left(1 - F_P\right)}{F_{c_P}\; F_P} + \frac{1 + M\; F_P}{F_{c_S}\;(1 - F_P)}\left(\frac{F_{r_S}}{F_{r_P}}\right)\right] \tag{4.21.a}$$

where :

$$M = \frac{\pi}{l_{em}}\sqrt{\frac{F_W}{F_h}}\,\sqrt{S_{Fe}} \tag{4.21.b}$$

The expression 4.21.a has a minimum for :

$$F_{P_{opt}} = \frac{1}{1 + \sqrt{\dfrac{F_{c_P}\left(1+M\right)}{F_{c_S}\left(1-M\right)}\left(\dfrac{F_{r_S}}{F_{r_P}}\right)}} \tag{4.22}$$

therefore , from eq. 4.5 , the optimal current density ratio is :

$$\frac{\sigma_P}{\sigma_S} = \sqrt{\frac{F_{c_S}\left(1+M\right)}{F_{c_P}\left(1-M\right)}\left(\frac{F_{r_S}}{F_{r_P}}\right)} \tag{4.23}$$

For square section scrapless lamination cores, with $F_{c_S} = F_{c_P}$ and $F_{r_S} = F_{r_P}$ the optimal values are :

$$F_{P_{opt}} = 0.43 \quad \text{and} \quad \sigma_P/\sigma_S = 1.34 \ .$$

Adopting these values P_{Cu} becomes 28 % lower with respect to the case corresponding to stacked windings with $F_P = 0.5$ and $\sigma_P = \sigma_S$. Nevertheless, adopting

F_P for minimal losses implies , as disadvantage, one higher current density in the inner winding , which has the worst heat transfer capability. By this reason , equal current densities are often adopted , even if this selection leads away of the optimum value from the winding losses point of view.

In a similar fashion as done with the shared coil-former case an equivalent turn factor (F_{le}) may be defined keeping the Joule losses still given by eq. 4.12 . For this purpose it must be :

$$F_{le} = \frac{1}{2}\left[1 - M\left(1 - F_P\right) + \frac{F_{c\,P}}{F_{c\,S}}\,\frac{F_{r_S}}{F_{r_P}}\,\frac{F_P\left(1 + M\ F_P\right)}{\left(1 - F_P\right)}\right] \quad (4.24)$$

(where *M* is defined by 4.21.b).

For the particular case with $F_{c\,S} = F_{c\,P}$ and $F_{r_S} = F_{r_P}$, adopting $F_P = 0.5$ yields :

$$F_{le} = 1 \quad (4.25)$$

For square section scrapless laminations with $F_P = F_{P_{opt}}$ it results : $F_{le} = 0.84$.

For E ferrite cores with the following typical dimensions :

$$A = C \quad ; \quad B = 1.5\ A \quad ; \quad H = 1.5\ A$$

one obtains ,

$$F_{P_{opt}} = 0.4 \quad \text{and} \quad F_{le}\Big]_{F_{P_{opt}}} = 0.77$$

(always with $F_{c\,S} = F_{c\,P}$ and $F_{r_S} = F_{r_P}$).

V. CURRENT DENSITY ADOPTION

A. Thermal considerations. Dissipation of losses

For temperature rises ranging about 50 ºC , assuming an ambient temperature of 40 ºC , the power dissipated by radiation may be estimated as :

$$\frac{P_{r[\mathrm{W}]}}{S_{dis\left[\mathrm{m}^2\right]}} = 7.08\ \Delta\theta_{[^\circ\mathrm{C}]} \quad (5.1)$$

(linear approximation obtained from the Stefan-Boltzmann [15] equation assuming an emissivity coefficient of 0.8).

On the other hand , the power dissipated by natural convection may be approximated through [15] :

$$\frac{P_{c[\mathrm{W}]}}{S_{dis\left[\mathrm{m}^2\right]}} = 2.17\ \Delta\theta_{[^\circ\mathrm{C}]}^{\ 1.25} \quad (5.2)$$

(valid for bodies with dimensions smaller than 0.5 m).

Therefore , the total dissipated power is :

$$\frac{P_{t[\mathrm{W}]}}{S_{dis\left[\mathrm{m}^2\right]}} = \left[7.08 + 2.17\ \Delta\theta_{[^\circ\mathrm{C}]}^{\ 0.25}\right]\Delta\theta_{[^\circ\mathrm{C}]}$$

and always assuming $\Delta\theta = 50\ ^\circ\mathrm{C}$, the above equation leads to the estimative expression :

$$\Delta\theta_{[^\circ\mathrm{C}]} = 0.0778\,\frac{P_{t[\mathrm{W}]}}{S_{dis\left[\mathrm{m}^2\right]}} \cong 780\,\frac{P_{t[\mathrm{W}]}}{S_{dis\left[\mathrm{cm}^2\right]}} \quad (5.3)$$

(linear equation valid only in the near range of $\Delta\theta = 50\ ^\circ\mathrm{C}$, rising over 40 ºC ambient temperature).

In case of E type cores the surface of heat dissipation is composed by one part corresponding to the coil windings $S_{dis_{Cu}}$ and other one $S_{dis_{Fe}}$ concerning to the core. For example, for square section scrapless laminated cores , from fig. 3.a and c , one obtains :

$$S_{dis_{Cu}} = \left(5 + 2\pi\right)A^2 \quad , \quad S_{dis_{Fe}} = 14.5\ A^2$$

and the total dissipation surface becomes :

$$S_{dis_{tot}} = S_{dis_{Cu}} + S_{dis_{Fe}} = \left(19.5 + 2\pi\right)A^2 = 25.8\ A^2 \quad (5.4)$$

Defining the thermal resistance as :

$$R_\theta = \frac{\Delta\theta}{P_t} \quad (5.5)$$

from eqs. 5.3 and 5.4 it results :

$$R_{\theta\ tot}\left[^\circ\mathrm{C/W}\right] \cong \frac{30}{\left(A_{[\mathrm{cm}]}\right)^2} \quad (5.6)$$

This expression may be used to estimate the transformer temperature rise when the copper and iron losses cause similar rises. Notice that $S_{dis_{Cu}}$ and $S_{dis_{Fe}}$ are similar areas. Therefore, when the core and winding losses are similar, the temperature rise will be comparable , and the approximation made will be acceptable.

In other circumstances , it will be suitable to verify the coil and core temperature rise separately, assuming isolated dissipations paths and using each kind of loss with its own dissipation area. It should be ensured that the highest temperature rise computed be lower than the maximum specified.

The thermal conduction resistance between coil and core is usually high because the coil former is plastic made and an air filled gap lies between the coil former and the core central leg.

As usually P_{Cu} and P_{Fe} are similar, so they are $S_{dis_{Cu}}$ and $S_{dis_{Fe}}$, the core and coil temperature rise become similar. Therefore, stated the thermal resistance is high, the heat conduction exchange between coil and core must be neglectible in a first trial approximation.

Example :

From the transformer thermal model [16] depicted in fig. 4 , one concludes :

$$P_{Cu/Fe} = \frac{P_{Cu}\ R_{\theta_{Cu}} - P_{Fe}\ R_{\theta_{Fe}}}{R_{\theta_{Cu/Fe}} + R_{\theta_{Cu}} + R_{\theta_{Fe}}} \quad (5.7)$$

Utilizing a core E42-15 , with 230 turns of 0.60 mm wire the D.C. resistance results : $R_{DC} = 1.3\,\Omega$.

Applying a direct current of 1.13 A the temperature rise measured was $\Delta\theta = 26\ ^\circ\mathrm{C}$ when vertical mounted, and 33 ºC if horizontal mounted. Therefore, the average value $\Delta\theta = 29.5\ ^\circ\mathrm{C}$ will be adopted for calculation purposes.

From equations deduced for $S_{dis_{Cu}}$ and $S_{dis_{Fe}}$:

$R_{\theta_{Cu}} = 24.2\ ^\circ\mathrm{C/W}$ and $R_{\theta_{Fe}} = 17.6\ ^\circ\mathrm{C/W}$.

From the model shown in fig. 4 (with $P_{Fe} = 0$) the total equivalent thermal resistance becomes :

$$R_{\theta_{eq\ tot}} = \frac{1}{\frac{1}{R_{\theta_{Cu}}} + \frac{1}{R_{\theta_{Cu/Fe}} + R_{\theta_{Fe}}}} = \frac{\Delta\theta}{{I_{DC}}^2\ R_{DC}} \qquad (5.8)$$

from which :

$$R_{\theta_{Cu/Fe}} = \frac{1}{\frac{{I_{DC}}^2\ R_{DC}}{\Delta\theta} - \frac{1}{R_{\theta_{Cu}}}} - R_{\theta_{Fe}} \qquad (5.9)$$

and using the above estimated values for $R_{\theta_{Cu}}$ and $R_{\theta_{Fe}}$, this gives $R_{\theta_{Cu/Fe}} = 49.7\ ^{o}\mathrm{C/W}$.

Assuming a typical case where $P_{Cu} = P_{Fe} = \frac{P_{tot}}{2}$, eq. 5.7 yields :

$$\frac{P_{Cu/Fe}}{P_{tot}} = \frac{1}{2}\left(\frac{R_{\theta_{Cu}} - R_{\theta_{Fe}}}{R_{\theta_{Cu/Fe}} + R_{\theta_{Cu}} + R_{\theta_{Fe}}}\right) \qquad (5.10)$$

thus, for the above experimental values, eq. 5.10 gives : $P_{Cu/Fe} = 0.036\ P_{tot}$ which allows, in first instance, to neglect the thermal exchange between the core and the coil.

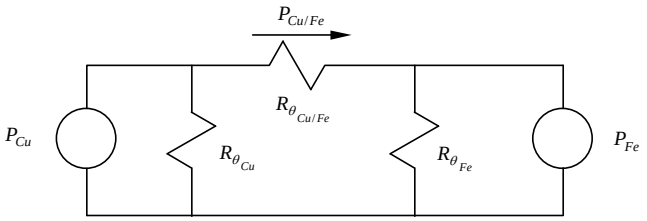

Figure 4 : Thermal model of an open-core transformer (C , E , EC or RM type cores).

B. Loss balance between core and coil [3] [7] [8] [14]

The iron losses may be estimated by [6][12][18] :

$$P_{Fe} = k_{Fe}\ f^{\xi}\ {B_m}^{\beta}\ V_{Fe} \qquad (5.11)$$

where for most ferrites : $\xi = 1.3$ and $2 \le \beta \le 2.7$ being $\beta \cong 2$ for high permeability materials aimed for switching frequencies ranging from 20 to 40 kHz , and $\beta \cong 2.5$ for low permeability ferrites suitable for higher frequencies.

Depending on the switching frequency the material choice should be done using the loss charts available from ferrite manufacturers [6][9][10].

The copper losses may be expressed by eq. 4.12 (with F_{le} defined by eq. 4.11 or 4.24 , depending on the winding structure).

Obtaining n_P from eq. AII.2 (see Appendix II) and substituting into eq. 4.12 , yields:

$$P_{Cu} = 2\rho_{eq_P}\left(\frac{V_{P_{ef}}\ I_{P_{ef}}}{k_C\ f_{fV}\ f}\right)^2 \frac{F_{le}\ l_{em}}{F_P\ F_{c_P}\ F_W\ {S_{Fe}}^3}\ \frac{1}{{B_m}^2} = \frac{K_{Cu}}{{B_m}^2} \qquad (5.12)$$

The total losses are the sum of the core losses plus the windings ones , becoming a function of B_m which should be adopted looking for minimal total losses [14].

According to eqs. 5.11 and 5.12 :

$$P_{tot} = P_{Fe} + P_{Cu} = K_{Fe}\ {B_m}^{\beta} + \frac{K_{Cu}}{{B_m}^2} \qquad (5.13)$$

expression that has a minimum for :

$$2\ K_{Cu} \big/ {B_m}^2 = \beta\ K_{Fe}\ {B_m}^{\beta} \qquad (5.14)$$

which leads to the optimal condition :

$$P_{Cu} = \frac{\beta}{2}\ P_{Fe} \qquad (5.15)$$

Notice that only if $\beta = 2$ then $P_{Cu} = P_{Fe}$ which is the optimal condition. However, even if $\beta = 2.6$, the optimal values of P_{Cu} and P_{Fe} are not quite different.

C. Current density adoption as function of temperature rise

1. Transformers: General expression

Assuming winding and core losses of the same order , and provided similar dissipation surfaces , the final temperatures will resemble.

Therefore, given a high winding-core thermal resistance , the heat exchange will be small enough to assume that the windings will dissipate only through the air-exposed coil surface , this should be the area used for calculations ($S_{dis_{Cu}}$). According to the nomenclature of fig. 3.a :

$$S_{dis_{Cu}} = 2\left(\pi\ C + A\right)H + 4\left(\frac{\pi}{2}\ C^2 + A\ C\right) \qquad (5.16)$$

With definitions 4.17 and eq. 4.19 :

$$\frac{S_{dis_{Cu}}}{S_{Fe}} = 2\ \pi\ F_W\left[1 + \frac{1}{F_h} + \frac{2 + F_h}{\pi\sqrt{F_W\ F_s\ F_h}}\right] \qquad (5.17)$$

The effective value of the primary current may be expressed as function of the current density by eqs. 2.7 and 2.8 as :

$$I_{P_{ef}} = \sigma_P\ S_{Cu_P} = \sigma_P\ F_{c_P}\ F_P\ F_W\ \frac{S_{Fe}}{n_P} \qquad (5.18)$$

that substituted into eq. 4.12 gives :

$$P_{Cu} = 2\rho_{eq_P}\ {\sigma_P}^2\ F_{c_P}\ F_P\ F_W\ F_{le}\ l_{em}\ S_{Fe} \qquad (5.19)$$

where F_{le} depends on the the winding structure (given by eqs. 4.11 or 4.24) , but in most cases adopting $F_{le} \cong 1$ may be an acceptable first trial approximation.

From fig. 3.b , using eq. 4.16 yields l_{em} , and utilizing the definitions 4.17 and eq. 4.19 it results :

$$l_{em} = \left[2\frac{\left(1 + F_s\right)}{\sqrt{F_s}} + \pi\sqrt{\frac{F_W}{F_h}}\right]\sqrt{S_{Fe}} \qquad (5.20)$$

Substituting eq. 5.20 into 5.19 :

$$P_{Cu} = 2\rho_{eq_P}\ {\sigma_P}^2\ F_{c_P}\ F_P\ F_W\ F_{le} \cdot \left[2\frac{\left(1 + F_s\right)}{\sqrt{F_s}} + \pi\sqrt{\frac{F_W}{F_h}}\right]\ {S_{Fe}}^{3/2} \qquad (5.21)$$

Substituting eqs. 5.21 and 5.17 into 5.3 yields :

$$\Delta\theta = 0{,}078\rho_{eq_P}\ {\sigma_P}^2\ F_{c_P}\ F_P\ F_{le}\left[\frac{\frac{\left(1 + F_s\right)}{\pi\sqrt{F_s}} + \frac{1}{2}\sqrt{\frac{F_W}{F_h}}}{1 + \frac{1}{F_h} + \frac{2 + F_h}{\pi\sqrt{F_W\ F_s\ F_h}}}\right]\sqrt{S_{Fe}}$$

(5.22)

from which one obtains :

$$\sigma_{P}\left[\mathrm{A}/\mathrm{mm}^2\right] = 0{,}358\sqrt{\frac{\Delta\theta\left[^{\circ}\mathrm{C}\right]}{\rho_{eq_P}\left[\mu\Omega\,\mathrm{cm}\right]}}\;\frac{F_{gm}}{\sqrt{F_P\;F_{c_P}\;F_{le}}}\;\frac{1}{\sqrt[4]{S_{Fe}\left[\mathrm{cm}^2\right]}} \tag{5.23.a}$$

where F_{gm} is a core geometry dependent factor :

$$F_{gm} = \sqrt{\frac{1+\frac{1}{F_h}+\frac{2+F_h}{\pi\sqrt{F_W\;F_s\;F_h}}}{\frac{\left(1+F_s\right)}{\pi\sqrt{F_s}}+\frac{1}{2}\sqrt{\frac{F_W}{F_h}}}} \tag{5.23.b}$$

For example, for square section scrapless lamination cores, assuming a temperature rise of 50 ºC and $\rho_{eq_P} = 20\;\mu\Omega\,\mathrm{cm}$, the following estimative expression is obtained :

$$\sigma_{P}\left[\mathrm{A}/\mathrm{mm}^2\right] \cong \frac{5}{\sqrt{A\left[\mathrm{cm}\right]}}$$

classical empirical formula well known by craftsmen, where *A* is the central leg width.

2. Ferrite made chokes

In this particular case, it is possible to find from manufacturer tables A_R such as :

$$R_{Cu} = A_R\;n^2 \tag{5.24}$$

Usually $A_R\big]_{0.5}$ is specified as the A_R value corresponding to $F_c = 0.5$ [6]. Therefore :

$$A_R = \frac{A_R\big]_{0.5}}{2\;F_c} \tag{5.25}$$

The copper losses may be estimated by :

$$P_{Cu} = {I_{ef}}^2\;R_{Cu} = \sigma^2\;{S_{Cu}}^2\;A_R\;n^2 \tag{5.26}$$

where :

$$S_{Cu} = F_c\;\frac{S_W}{n} = F_c\;F_W\;\frac{S_{Fe}}{n} \tag{5.27}$$

Substituting 5.25 and 5.27 into 5.26 yields :

$$P_{Cu} = \sigma^2\;{S_{Fe}}^2\;{F_W}^2\;\frac{F_c}{2}\;A_R\big]_{0.5} \tag{5.28}$$

Neglecting the iron losses (respect to the copper ones) it may be assumed that :

$$P_{Cu} = \Delta\theta / R_{\theta_{tot}} \tag{5.29}$$

Equating expressions 5.28 and 5.29 yields :

$$\sigma\left[\frac{\mathrm{A}}{\mathrm{mm}^2}\right] = \frac{10}{F_W\;S_{Fe}\left[\mathrm{cm}^2\right]}\sqrt{\frac{2\;\Delta\theta\left[^{\circ}\mathrm{C}\right]}{R_{\theta_{tot}}\left[^{\circ}\mathrm{C/W}\right]\;F_c\;A_R\big]_{0.5}\left[\mu\Omega\right]}} \tag{5.30}$$

Notice that eq. 5.30 do not consider the resistance rise due to both the skin and proximity effects. In most choke application cases, this is not important because the D.C. component is the main harmonic current component.

VI. VOLUMETRIC CORE COMPARISON BETWEEN FLYBACK AND FORWARD CONVERTERS

A. Volumetric ratio

The volume of a magnetic core is related to the effective length by ,

$$\boldsymbol{V}_{Fe} = S_{Fe_{ef}}\;l_{Fe} = \left(\frac{S_{Fe_{ef}}}{S_{Fe}}\right)S_{Fe}\;l_{Fe} = k_E\;S_{Fe}\;l_{Fe} \tag{6.1}$$

and the magnetic length is related to the geometric minimal core section by,

$$l_{Fe} = k_S\;\sqrt{S_{Fe}} \tag{6.2}$$

which yields :

$$\boldsymbol{V}_{Fe} = k_E\;k_S\;{S_{Fe}}^{3/2} = k_{SE}\;{S_{Fe}}^{3/2} \tag{6.3}$$

where :

$$k_{SE} = k_E k_S = S_{Fe_{ef}}\;l_{Fe}\Big/\sqrt{{S_{Fe}}^3}$$

For scrapless laminations k_E = 1 and k_S = 6 so k_{SE} = 6 , while for ferrite E cores k_{SE} usually lies between 5 and 7 [6][10] (as it may be calculated from core manufacturer data).

The required core volumes will be compared assuming equal shapes and proportions, so with the same k_{SE} .

The total volume occupied by the cores of the magnetic components of a forward converter is :

$$\boldsymbol{V}_{Fe_{FW}} = \boldsymbol{V}_{Fe_{TFW}} + \boldsymbol{V}_{Fe_L}$$

Then, the volumetric ratio for converter comparison may be defined as :

$$\Re\boldsymbol{V}_{FW/FB} = \frac{\boldsymbol{V}_{Fe_{FW}}}{\boldsymbol{V}_{Fe_{FB}}} = \frac{\boldsymbol{V}_{Fe_{TFW}} + \boldsymbol{V}_{Fe_L}}{\boldsymbol{V}_{Fe_{FB}}} \tag{6.4}$$

Substituting the aproximative form of the sizing equations 2.14 , 3.2 and 3.10 in the expression 6.3 and replacing the results in 6.4 yields :

$$\Re\boldsymbol{V}_{FW/FB} = \frac{\boldsymbol{V}_{Fe_{FW}}}{\boldsymbol{V}_{Fe_{FB}}} = \delta i_P^{3/4} + \left[\eta\;\frac{\left(1-D\right)}{\sqrt{D}}\;F_P\;\frac{\sigma_{I_P}}{\sigma_{I_L}}\right]^{3/4} \tag{6.5}$$

The most commonly partition factor adopted is $F_P = 0.5$. Assuming this partition value and $\sigma_P = \sigma_L$, the volumetric ratio is shown in figs. 5.a and 5.b with parameters D and δi_P for $\eta = 1$. Obviously, when $\Re\boldsymbol{V}_{FW/FB} < 1$ the forward topology must be preferred.

B. Power switch sizing considerations

The profit factor (or power utilization ratio) of the power device is defined as :

$$f_{pr} = \frac{P_O}{P_D}$$

where P_O is the maximum available output power of the converter and P_D is the rated switching power for the power device. The profit factor becomes better in continuous operation mode and it may be easily demonstrated that for both topologies it results :

$$f_{pr} = \eta\;D\left(1-D\right)\left(1-\frac{\delta i_P}{2}\right) \tag{6.6}$$

The profit factor becomes maximum when $D = 0.5$. In this case, if $\eta = 1$ the former expression yields :

$$f_{pr} = \frac{1}{4}\left(1 - \frac{\delta i_P}{2}\right) \tag{6.7}$$

Substituting 6.7 in 6.5 , for $F_P = 0.5$:

$$\Re \boldsymbol{V}_{FW/FB} = \left[2\left(1 - 4\ f_{pr}\right)\right]^{3/4} + 2^{-9/8} \tag{6.8}$$

In accordance with 6.6 it must be :

$$\frac{1}{8} \le f_{pr} \le \frac{1}{4} \tag{6.9}$$

so from 6.8 it results :

$$0.458 < \Re \boldsymbol{V}_{FW/FB} < 1.46 \tag{6.10}$$

The boundary value for the profit factor is

$$f_{pr_{lim}} = 0.195 \cong 0.2 \ .$$

Actually, the adoption $\sigma_P = \sigma_L$ may be too conservative, because the core for the inductor usually results smaller than the one required for the transformer. Therefore, the inductor can dissipate heat better than the transformer due to its higher *surface/volume* ratio. Also, the inductor core power losses are lower, since the hysteresis loop there is smaller than the one performed in the transformer. Consequently, higher copper losses (per volume) should be admissible, allowing higher current density on inductor windings (according to eq. 5.30).

The inductor current density is usually adopted between $\sigma_P \le \sigma_L \le 1.5\sigma_P$. A higher current density reduces the inductor volume but degrades the efficiency and complicates the close loop converter operation making the voltage transfer ratio a function of the output load.

Using $\sigma_L = 1.5\,\sigma_P$ and recalculating the boundary value for the profit factor yields, $f_{pr_{lim}} = 0.209$, so the aproximative value 0.2 is again valid.

VII. CONCLUSIONS

The widely used stacked winding technique allows partition factors others than 1/2 if required , but usually , the inner winding density current has to be limited to values such as the optimal efficiency cannot be achieved. However, these kind of windings have smaller leakage inductance than shared coil-former made, but they present a bigger interwinding capacity and poorer isolation features.

Therefore, even if the secondary was allocated in a separated coil-section, the demagnetizing coil should be placed over the primary winding to ensure a good magnetic coupling. In battery powered converters, bifilar winding will improve the magnetic coupling. In off-line SMPS bifilar windings are not reliable enough [7] and a good practice should be to interpose the primary between both the halved demagnetizing winding sections . This increases the parasite interwinding capacity [12] but an appropriate connection of the demagnetizing diode may overcome this drawback [7].

For $f_{pr} > f_{pr_{lim}}$ the forward topology requires small core volume than the flyback one and vice versa, so for $f_{pr} < f_{pr_{lim}}$ a flyback implementation should be preferred. When the selected operation duty cycle is near the optimal value 0.5 , adopting σ_L higher than σ_P does not change the boundary value obtained.

Assuming D as the maximum duty cycle for nominal output power, the maximum voltage over the power switch will be : $V_{CE_{max}} = V_P / (1 - D)$ expression valable for both topologies here involved. Using this equations with 6.5 and 6.6 , $\Re \boldsymbol{V}_{FW/FB}$ is plotted in fig. 5.c , as function of f_{pr} with the parameter $V_{CE_{max}} / V_P$. There, the most suitable operation area for each topology are marked.

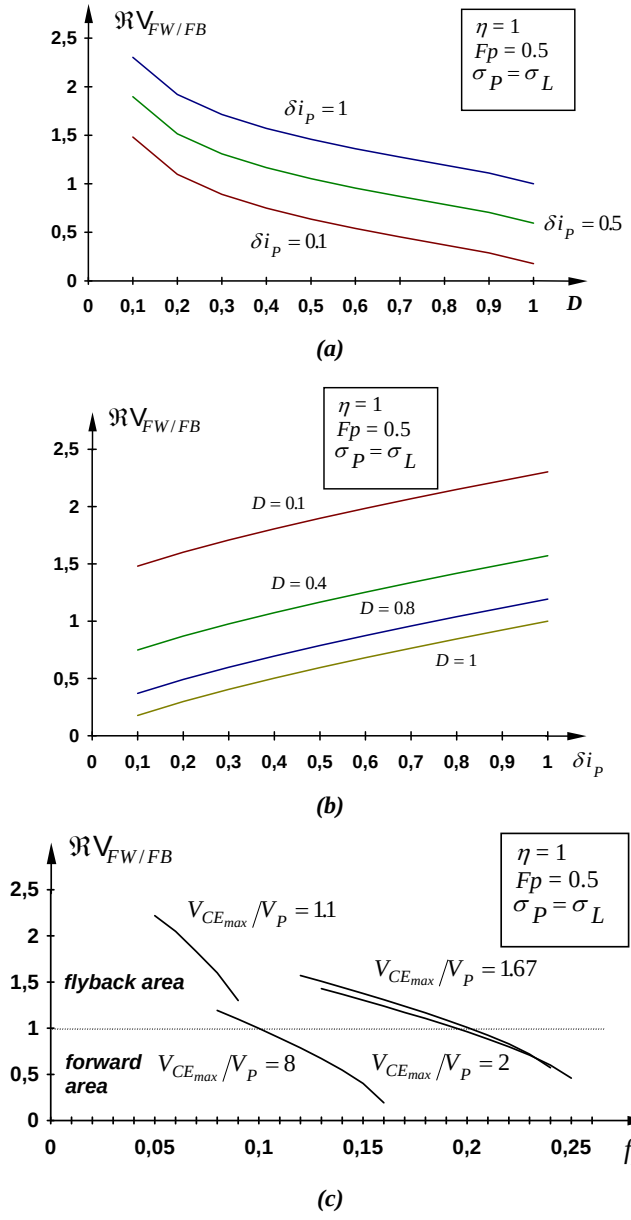

Figure 5 : Volume ratio as function of *(a)* duty-cycle, *(b)* primary current increment and *(c)* device profit factor.

APPENDIX I : Magnetic flux density adoption

A. Maximum efficiency selection

For the optimal condition stated by eq. 5.15 the total losses become :

$$P_{tot} = P_{Cu} + P_{Fe} = \left(1+\frac{\beta}{2}\right) P_{Fe} = k_{Fe}\ f^{\xi}\ B_m{}^{\beta} \left(1+\frac{\beta}{2}\right) \mathcal{V}_{Fe} \tag{AI.1}$$

and the temperature rise may be estimated through :

$$\Delta\theta = P_{tot}\ R_{\theta_{tot}} \tag{AI.2}$$

From eqs. AI.1 and AI.2 it results :

$$B_m\big]_{opt} = \left[\frac{\Delta\theta \Big/ R_{\theta_{tot}}}{k_{Fe}\ f^{\xi} \left(1+\frac{\beta}{2}\right) \mathcal{V}_{Fe}} \right]^{1/\beta} \tag{AI.3}$$

For most ferrite cores , this value is smaller than the maximum allowable (which depends on the switching frequency adopted). Therefore, a higher flux density might be adopted to increase the available output power at price of an efficiency degradation.

B. Maximum output power selection

In this case, the current density will be adopted as function of the temperature rise (see section V - C).

For a given core, once the current density was adopted, P_{Cu} becomes determinated from eq. 5.19 . For these copper losses , it should be avoided that the core temperature rise surpasses the maximum specified for the coil , in order to prevent an additional heat transfer to the windings. Consequently , it must be :

$$\frac{P_{Cu}}{S_{dis_{Cu}}} = \frac{P_{Fe}}{S_{dis_{Fe}}} \tag{AI.4}$$

Being both temperature rises identical :

$$\Delta\theta = \left(P_{Cu} + P_{Fe} \right) R_{\theta_{tot}} \tag{AI.5}$$

From eqs. AI.4 and AI.5 it results :

$$P_{Fe} = \frac{\Delta\theta}{R_{\theta_{tot}}} \left(\frac{S_{dis_{Fe}}}{S_{dis_{tot}}} \right) \tag{AI.6}$$

Using eqs. 5.11 and AI.6 , one obtains :

$$B_m\big]_{Po_{max}} = \left[\frac{\frac{\Delta\theta}{R_{\theta_{tot}}} \left(\frac{S_{dis_{Fe}}}{S_{dis_{tot}}} \right)}{k_{Fe}\ f^{\xi}\ \mathcal{V}_{Fe}} \right]^{1/\beta} \tag{AI.7}$$

Relating the expressions AI.3 and AI.7 :

$$\frac{B_m\big]_{Po_{max}}}{B_m\big]_{opt}} = \left[\left(\frac{S_{dis_{Fe}}}{S_{dis_{tot}}} \right) \left(1+\frac{\beta}{2}\right) \right]^{1/\beta} \tag{AI.8}$$

For example, for a core E55-21 made with a material such as $\beta = 2.5$, $B_m\big]_{Po_{max}}$ becomes approximately 14 % greater than $B_m\big]_{opt}$.

Using the B_m adoption criteria stated by eqs. AI.3 or AI.7 requires a previously made core selection, but it is just for selecting the core (as output power function) that B_m is first needed. To overcome this obstacle , one estimation a priori of B_m can be made based upon known reference values , through the equation deduced keeping constant the core density losses :

$$B_{m(f)} = \left(\frac{f_{ref}}{f} \right)^{\xi/\beta} B_{ref} \tag{AI.9}$$

For high permeability ferrites used from 10 to 50 kHz , the references may be $B_{ref} = B_{sat}$ and $f_{ref} = f_{min}$, where f_{min} is the minimum recommendable operating frequency, that is, the maximal switching frequency which allows using $B_m = B_{sat}$. Under f_{min} it should be preferable to adopt other material , while for $f > f_{min}$ it is necessary to reduce B_m according to eq. AI.9 .

Usually $\xi/\beta \cong 0.5$ so, the eq. AI.9 may be approximated as :

$$B_{m(f)} = \sqrt{\frac{f_{ref}}{f}}\ B_{ref} \tag{AI.10}$$

For low permeability ferrites suitable for high frequency switching , the reference values may be determined as function of temperature rise from manufacturer issued curves (or tables).

For example, suitable reference values for N27 and N47 materials are :

N27 : f_{ref} = 20 kHz ; B_{ref} = 0.2 T

N47 : f_{ref} = 100 kHz ; B_{ref} = 0.1 T .

APPENDIX II : Transformer core sizing equation

The Faraday law applied to a transformer magnetic circuit yields :

$$V_P = n_P\ S_{Fe}\ \frac{\Delta B}{\Delta t} \tag{AII.1}$$

For symmetrical converters $\Delta B = 2B_{max}$ and $\Delta t = D\,T/2$, while for continuous operating mode forward converters $\Delta B = B_{max} - B_r \cong B_{max}$ and $\Delta t = D\,T$, where B_r is the residual flux density (assumed that $B_r << B_{max}$ in soft magnetic materials).

On the other hand , in flyback converters :

$\Delta B = B_{max} - B_{min} = B_{max}\ \delta i_P$ and $\Delta t = DT$.

In symmetrical converters operating in continuous mode :

$V_{P_{ef}} = \sqrt{D}\,V_P$ and $V_{P_{av}} = D\,V_P$,

so the voltage form factor results :

$f_{f_V} = 1/\sqrt{D}$.

For asymmetrical converters operating in continuous mode :

$$V_{P_{ef}} = \sqrt{\frac{D}{1-D}}\,V_P \quad \text{and} \quad V_{P_{av}} = 2D\,V_P$$

therefore ,

$$f_{f_V} = \frac{1}{2\sqrt{D\left(1-D\right)}}$$

which allows expressing the eq. AII.1 as :

$$V_{P_{ef}} = k_C \; f_{f_V} \; n_P \; S_{Fe} \; B_m \; f \qquad \text{(AII.2)}$$

where :

$k_C = 4$ for symmetrical converters

$k_C = 2$ for forward converters

$k_C = 2\,\delta i_P$ for flyback converters

and the notation was simplified writing $B_m = B_{max}$.

Using eq. 5.18 the primary current may be expressed as density current function. Then , using eqs. AII.2 and 5.18 the primary apparent power is obtained :

$$V_{P_{ef}} \; I_{P_{ef}} = k_C \; f_{f_V} \; B_m \; f \;\; \sigma_P \; F_{c_P} \; F_P \; F_W \; S_{Fe}{}^2 \qquad \text{(AII.3)}$$

from which the minimal required core section (S_{Fe}) may be found.

The output power may be expressed as function of the apparent primary power, yielding :

$$P_O = \eta \;\; k_{u_T} \; V_{P_{ef}} \;\; I_{P_{ef}} \qquad \text{(AII.4)}$$

where k_{u_T} is the transformer utilization factor , defined as the ratio between the active primary power (or D.C. primary supply power) and the apparent primary power adopted for transformer design. Suitables design values are :

$k_{u_T} = \sqrt{1-D}$ for asymmetrical converters and

$k_{u_T} = 1$ for symmetrical ones.

Substituting AII.4 into AII.3 and rearranging , the required minimal core section is obtained as output power function :

$$S_{Fe} = \sqrt{\frac{P_O}{\eta \;\; k_{u_T} \; k_C \; f_{f_V} \; B_m \;\; f \;\; \sigma_P \; F_{c_P} \; F_P \; F_W}} \qquad \text{(AII.5)}$$

Examples:

For a ferrite core E42-15 made with material N27 , assuming $\Delta\theta = 30\,^{\circ}\mathrm{C}$ yields $\sigma_P = 3.1\ \mathrm{A/mm^2}$ (see section 4). Adopting the typical values : $D = 0.4$, $F_b = 0.36$, $F_P = 0.5$, $\eta = 0.9$, $f = 20$ kHz and $B_m = 0.2$ T , for the forward topology , from eqs. AII.4 and AII.5 , it results : $P_O = 100$ W , while the empirical manufacturer graphic [6] yields $P_O = 110$ W .

For an E55-21 core with the same material , adopting the same topology and working conditions, for equal temperature rise it should be $\sigma_P = 2.7\ \mathrm{A/mm^2}$, which yields $P_O = 272$ W , while from manufacturer data , $P_O = 275$ W .

APPENDIX III : Skin and proximity effects

For a single foil conductor subjected only to the skin effect, the increase of resistance is given by [20] :

$$k_{rS} = \frac{R_{ac}}{R_{dc}} = \frac{\xi}{2}\,\frac{\sinh\xi + \sin\xi}{\cosh\xi - \cos\xi} \qquad \text{(AIII.1)}$$

where:

$\xi = h/\Delta$

Δ : penetration depth , $\Delta = \sqrt{\rho \,/\, \pi \; f \; \mu_o}$

h : foil thickness

If the foil conductor is immersed into the magnetic field due to other conductors (proximity field) the resistance will rise even more [12][13].

Assuming the proximity field uniform over the conductor cross section, orthogonality appears between skin and proximity effects [20]. This decouples both effects and simplifies calculations [21].

For the foil conductor of the *m* layer the increase of resistance is given by :

$$\frac{R_{ac}}{R_{dc}} = \frac{\xi}{2}\left[\frac{\sinh\xi + \sin\xi}{\cosh\xi - \cos\xi} + (2m-1)^2\,\frac{\sinh\xi - \sin\xi}{\cosh\xi + \cos\xi}\right] \qquad \text{(AIII.2)}$$

The first term in eq. AIII.2 is identical to eq. AIII.1 and describes the skin effect.

For multilayer windings :

$$F_r = \frac{R_{ac}}{R_{dc}} = \frac{\xi}{2}\left[\frac{\sinh\xi + \sin\xi}{\cosh\xi - \cos\xi} + \left(\frac{4\,p^2-1}{3}\right)\frac{\sinh\xi - \sin\xi}{\cosh\xi + \cos\xi}\right] \qquad \text{(AIII.3)}$$

where p is the number of layers.

Therefore F_r may be expressed as :

$$F_r = k_{rS} + k_{rX} \qquad \text{(AIII.4)}$$

where k_{rS} is given by eq. AIII.1 and k_{rX} results :

$$k_{rX} = \frac{\xi}{2}\left(\frac{4\,p^2-1}{3}\right)\frac{\sinh\xi - \sin\xi}{\cosh\xi + \cos\xi} \qquad \text{(AIII.5)}$$

For $\xi \le 2$ the following approximations apply [12] :

$$k_{rS} \cong 1 \qquad \text{(AIII.6.a)}$$

and ,

$$k_{rX} \cong \frac{5\,p^2-1}{45}\,\xi^4 \qquad \text{(AIII.6.b)}$$

In order to extend this one-dimensional approach to round wire windings, Dowell [13] introduces an equivalent square conductor thickness from :

$$S_{Cu} = h^2 = \pi\left(\frac{d}{2}\right)^2 \quad \text{therefore ,} \quad h = \frac{\sqrt{\pi}}{2}\,d \qquad \text{(AIII.7)}$$

Each layer is supposed formed by n_l turns of square section equivalent conductors (fig. A3).

Since the square section conductors are separated by a gap *s* , a one-dimensional layer copper factor has to be defined as:

$$F_l = \frac{n_l}{b_W}\,h \qquad \text{(AIII.8)}$$

where,

b_W : overall winding breadth

h : equivalent conductor thickness

n_l : number of turns per layer

In order to adjust this model to the one-dimensional approach of the single-foil winding , the penetration depth must be modified due to the porosity of the winding layer which increases the effective resistivity.

Therefore, defining :

$$\rho_{ef} = \rho / F_l \qquad \text{(AIII.9)}$$

it yields,

$$\Delta_{ef} = \sqrt{\rho_{ef} / \pi\ f\ \mu_o} = \frac{\Delta}{\sqrt{F_l}} \qquad \text{(AIII.10)}$$

which leads to the effective value of ξ to be applied in F_r estimations in case of round wire windings :

$$\xi = \frac{\sqrt{F_l}\ h}{\Delta} = \frac{\sqrt{\pi}}{2}\sqrt{F_l}\ \frac{d}{\Delta} \qquad \text{(AIII.11)}$$

If the increase in resistance due to eddy currents is excessive, one alternative is to use bunched conductors or litz wires. Then :

$$h = \frac{\sqrt{\pi}}{2} D_{st}$$

(where D_{st} is the strand diameter) and $F_l \cong F_W$. However, when the number of turns is small, the adoption of foil windings usually gives lower ac resistances. The use of litz wire may be considered for multilayer winding applications ranging over 500 kHz .

For inductors carrying DC (choke applications) adopting $d/\Delta \le 2$ is suitable enough in discontinuous mode operating converters, while $d/\Delta \le 4$ is acceptable in continuous mode operation.

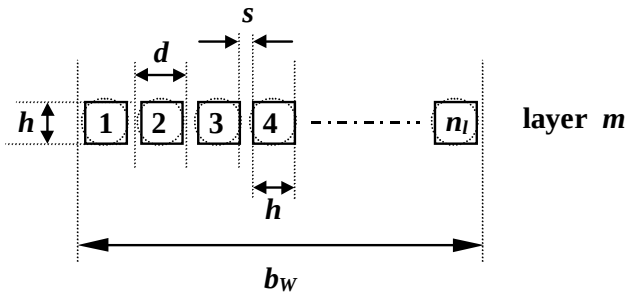

Figure A3 : A layer of square section conductors equivalent to one of round section conductors.

ACKNOWLEDGEMENT

The author would like to thank Prof. Carlos Christiansen for his interest and support that constantly encouraged this work.

REFERENCES

[1] R. Bausière , F. Labrique and G. Séguier, *Les convertisseurs de l'électronique de puissance. Tome 3: La conversion continu-continu*, Paris Fr. : Techn. et Doc. Lavoisier , 1987, Chap. 6 .

[2] J. P. Ferrieux , F. Forest , *Alimentations à découpage, convertisseurs à résonance* , Paris Fr. : Ed. Masson , 1987, Chap. 1 and 2.

[3] R. Tarter , *Solid-State Power Conversion Handbook* , N. York : Wiley-Interscience publ. , 1993 , Chap. 3 and 9.

[4] H. Tacca , *Convertidores asimétricos con doble transferencia directa e indirecta* , Tesis doctoral, Univ. de Buenos Aires, Fac. de Ingeniería, abril , 1998.

[5] C. R. Hanna, "Design of Reactances and Transformers Which Carry Direct Current", *AIEE Journal* , vol.46 , Febr. 1927 , p. 128 .

[6] Siemens, *Ferrites and Accesories. Data Book 90/91* , Berlin, Germany : Siemens Matsushita Components, 1990.

[7] K. H. Billings, *Switchmode Power Supply Handbook* , N. Y. : McGraw-Hill, 1989.

[8] A. I. Pressman, *Switching Power Supply Design* , N. Y.: McGraw-Hill, 1991.

[9] C. W. T. McLyman, *Transformer and Inductor Design Handbook* , N. Y. U.S.A. : M. Dekker, 1988.

[10] C. W. T. McLyman, *Magnetic Core Selection for Transformer and Inductors* , N. Y. U.S.A. : M. Dekker, 1997.

[11] H. E. Tacca, *Amélioration des caractéristiques des convertisseurs quasi-résonnants à transfert direct d'énergie* , Thèse doctorale, Univ. des Sciences et Technologies de Lille, France, avril 1993.

[12] E. C. Snelling, *Soft Ferrites, Properties and Applications* , London U. K. : London Iliffe Books, 1969.

[13] P. L. Dowell, "Effects of Eddy Currents in transformer Windings", *Proc. of the IEE* , vol. 113 , no. 8 , August 1966 , p. 1387 .

[14] A. Urling, V. Niemela, G. Skutt and T. Wilson, "Characterizing High-Frequency Effects in Transformer Windings - A Guide to Several Significant Articles", included in *Power Electronics Technology and Applications* , N. Y. U.S.A. : IEEE Press , 1993.

[15] M.I.T. E.E. staff, *Magnetic Circuits and Transformers*, Cambridge, U.S.A. : The MIT Press, 1943 , Chap. 8.

[16] R. Petkov, "Optimun Design of a High-Power, High-Frequency Transformer", *IEEE Trans. on Power Electronics*, vol. 11 , No. 1 , Jan. 1996 , p. 33.

[17] W. G. Hurley , W. H. Wölfle, and J. G. Breslin , "Optimized Transformer Design : Inclusive of High-Frecuency Effects", *IEEE Trans. on Power Electronics*, vol. 13 , No. 4 , July 1998 , p. 651.

[18] R. Boll (editor), *Soft Magnetics Materials: Fundamentals, Alloys, Properties, Products and Applications*, London, U.K. : Heyden, 1978.

[19] R. M. Bozorth, *Ferromagnetism* , N.Y. : IEEE Press, 1993.

[20] J. A. Ferreira, "Improved Analytical Modeling of Conductive Losses in Magnetic Components", *IEEE Trans. on Power Electronics*, vol. 9 , No. 1 , Jan. 1994 , p. 127.

[21] W. G. Hurley, W. H. Wölfle, and J. G. Breslin, "Optimized Transformer Design: Inclusive of High-Frequency Effects", *IEEE Trans. on Power Electronics*, vol. 13 , No. 4 , July 1998 , p. 651.

Hernán Emilio Tacca was born in Argentina on December 15, 1954. He received the B.E. degree in electrical engineering from the University of Buenos Aires (Argentina), in 1981 and the M.S. and Ph.D. degrees from the University of Sciences and Technologies of Lille (France) in 1988 and 1993 , respectively. In 1998 he received the Doctorate degree from the University of Buenos Aires. Since 1984 , he has been with the Faculty of Engineering of the University of Buenos Aires, where he is currently Assistant Professor and engaged in teaching and research in the areas of industrial electronics. His research interest are in the field of SMPS, UPS, battery chargers, soft-switching techniques and microcontroller control of power converters.